



## Segmentation of copper alloys processed by equal-channel angular pressing

Omid NEJADSEYFI<sup>1</sup>, Ali SHOKUHFAR<sup>1</sup>, Vahid MOODI<sup>2</sup>

1. Advanced Materials and Nanotechnology Research Lab, Faculty of Mechanical Engineering, K. N. Toosi University of Technology, Tehran, Iran;
2. Young Researchers and Elites Club, Birjand Branch, Islamic Azad University, Birjand, Iran

Received 11 October 2014; accepted 10 February 2015

**Abstract:** This research provides experimental evidence for localized shear, billet cracking, and segmentation during the processing of various copper alloys. The results demonstrate that although many parameters affect the shear localization, there is a direct relation between segmentation and alloy strength (hardness) that is related to the alloying elements and constitutive phases. For instance, alpha brass is successfully processed by ECAP at room temperature, but alpha/beta brasses fail even at a temperature of 350 °C. Finite element simulation of cracking and segmentation was performed using DEFORM<sup>TM</sup> to investigate the influence of different parameters on segmentation. The results confirm that friction and processing speed have narrow effects on attaining a perfect billet. However, employing back pressure could be reliably used to diminish shear localization, billet cracking, segmentation, and damage. Moreover, diminishing the flow localization using back pressure leads to uniform material flow and the billet homogeneity increases by 36.1%, when back pressure increases from 0 to 600 MPa.

**Key words:** back pressure; brass; bronze; damage; flow localization; stress–strain behavior; tensile strength; ductility

### 1 Introduction

The grain size of a polycrystalline metal is directly affecting its mechanical properties. At low temperatures, the strength is related to the grain size through the Hall–Petch relationship, which is of the form:

$$\sigma_y = \sigma_0 + k_y d^{-1/2} \quad (1)$$

where  $\sigma_y$  is the yield stress,  $\sigma_0$  is the friction stress,  $d$  is the average grain size, and  $k_y$  is a constant value of yielding. This equation demonstrates that reducing the grain size is beneficial for increasing the strength of the material. In addition, reducing the grain size enhances the superplastic formability of materials [1,2].

Grain refinement through the application of thermo-mechanical treatment leads to the grain sizes in the order of a few microns. However, these procedures cannot refine the grains up to the submicrometer (0.1 to 1.0  $\mu\text{m}$ ) or nanometer (<100 nm) range. To achieve ultra-fine grain size, it is necessary to use alternative techniques, in which materials are subjected to severe plastic deformation (SPD) without incurring any significant change in the overall dimensions of the work-

piece. Processing of alloys and metals through the SPD methods is attractive because it introduces significant grain refinement in bulk solids. Among various SPD techniques, equal-channel angular pressing (ECAP) has attracted much attention than other SPD methods in the last decade. Easy configuration, low cost, and the ability to produce relatively large samples of bulk ultrafine-grained and nanostructured materials are the most important advantages of this process [3]. In ECAP, a sample in the form of a rod or bar is pressed repetitively through a die to impose high strain to the work-piece. Some materials, specifically those having hexagonal close-packed crystal structure, are difficult to process by ECAP due to the limited number of slip systems. Such materials are prone for shear localization, segmentation and multiple cracking when they are pressed at room temperature [4]. These problems may be limited or even avoided by increasing the processing temperature and/or changing the channel angle within the die [5]. However, increasing the pressing temperature leads to larger grain sizes.

As the aim of the ECAP process is grain refinement together with the producing materials without defects, cracks, and segments, several procedures have been

adopted to avoid the development of shear bands and deformation inhomogeneity during the process. These procedures include using ECAP dies having angles larger than  $90^\circ$ , performing the process with low speed, increasing the processing temperature, using preliminary deformation step, and incorporating back pressure into the pressing operation. This research was conducted to reveal the damage evolution during processing various grades of copper alloys, and to provide experimental evidence for the occurrence of cracks, segmentation and shear localization in ECAP. However, considering cost, time, and availability of experimental procedures leads to concentrate on the numerical methods to assess the influence of different parameters in the ECAP process. In addition, less attention has been made on using finite element analysis (FEA) to predict damage, and segmentation in the literature. Among available reports, FIGUEIREDO et al [6] used FEA to evaluate the evolution of damage in an aluminum-based alloy. The analysis demonstrated that the cracks might be formed in the interiors of materials with strain hardening behavior (annealed sample) and the propagation of those cracks led to billet segmentation. Conversely, in near perfect plastic behavior (the samples processed by ECAP), there might be superficial cracking on the upper surfaces of the billets. However, those cracks were reasonably stable. They studied the effect of strain-rate sensitivity and die angle on the segmentation using numerical simulations and concluded that billet cracking and segmentation might be reduced in difficult-to-work alloys by increasing the strain-rate sensitivity and/or by increasing the channel angle within the die [7]. Generally, most of the studies dealing with ECAP, and specifically those related to flow localization in ECAP, concentrate on the materials such as titanium and magnesium. Therefore, in order to expand the current knowledge in this field, the effects of different processing parameters on the flow localization of Cu-based alloys were dealt using finite element analysis (FEA) and experimental tests.

## 2 Experimental

In this work, the ECAP process was conducted on five commercial Cu-based alloys as specified in Table 1. Free machining brass (also known as architectural bronze), and forging brass are categorized in alpha/beta alloys with more than 37% zinc. However, forging brass, containing less than 37% zinc is classified as alpha brass. Phosphor bronze, or tin bronze, is an alloy containing copper, tin, and phosphorous. Tin remains in the alpha copper solid solution and the phosphorus forms copper phosphide phase. When the content of tin is above 10%, as shown in the copper–tin phase diagram, a second

phase is formed, which is brittle. Furthermore, gear bronze has a strong bronze matrix (alpha phase) with a fine dispersion of the hard delta phase, which improves the strength of the alloy.

**Table 1** Specifications of processed materials by ECAP

Alloy No.	Name	UNS number	Nominal composition	Vickers microhardness
A	Free machining brass	C38500	Cu–39%Zn–3%Pb	147
B	Gear bronze	C92900	Cu–10%Sn–3.5%Ni–2.5%Pb	128
C	Forging brass	C37700	Cu–39%Zn–2%Pb	105
D	Phosphor bronze	C51000	Cu–10%Sn–0.25%P	93
E	Cartridge brass	C26000	Cu–30%Zn	86

To conduct ECAP on the above-mentioned materials, all samples were cut and machined to be 10 mm in diameter and 40 mm in length. Prior to ECAP, annealing heat-treatment was performed for all samples by keeping the billets at  $500^\circ\text{C}$  for 3 h and then letting them to cool down to room temperature.

The ECAP process was performed at room temperature through a single pass with a pressing speed of 10 mm/s. In the case of sample failure, the temperature was increased up to  $350^\circ\text{C}$  to repeat the process. A closed die made of H13 steel with a cross-channel angle ( $\Phi$ ) of  $90^\circ$  between the vertical and horizontal channels and an outer corner angle ( $\Psi$ ) of  $20^\circ$  was used. A heater was incorporated within the die to control the temperature. In addition, graphite powder was used as lubricant during ECAP process.

The Vickers microhardness values were measured using Shimadzu Type M microhardness tester with a load of 0.49 N for a dwell time of 10 s. Furthermore, the tensile tests were performed on the specimens, prepared from longitudinal direction of the samples, with 5 mm in gage diameter, and 25 mm in gage length employing an initial strain rate of  $0.01\text{ s}^{-1}$ .

Optical microscopy and scanning electron microscopy were used to observe the microstructure of the annealed and processed billet. For this purpose, the billets were cold-mounted in epoxy and surface preparation was conducted by grinding the samples using 100, 240, 400, 600, 1200, 2000, and 3000 grit SiC papers and then by employing alumina polishing powder. Then, the billets were chemically etched in a solution of  $\text{FeCl}_3$ , HCl, and  $\text{C}_2\text{H}_5\text{OH}$  (3 g, 10 mL, and 90 mL, respectively) at room temperature for 15 s.

### 3 Numerical simulation

To conduct FE simulations, DEFORM™ Ver 10.0 was employed. The die and punch were assumed to be rigid and the billet was assumed as an elastic-plastic object. The punch speed was chosen as 10 mm/s. A  $d10\text{ mm} \times 40\text{ mm}$  billet was meshed to approximately 8000 four-noded elements using automatic remeshing to regenerate the distorted elements during the simulations. The convergence condition was satisfied with this number of elements, and the results were independent from the number of the meshes. A back punch was also modeled to exert back pressure during the process when needed.

As the main reason of simulations predicting billet cracking, shear localization, and segmentation, normalized Cockcroft&Latham criterion was used as an appropriate damage criterion. This criterion has been extensively used to predict the fracture and damage evolution during metalworking processes [8,9]. As normalized Cockcroft&Latham fracture criterion satisfies the requirements of large plastic deformation problems, it can be reliably used to predict the damage in ECAP. Normalized Cockcroft&Latham criterion is then given by [10]

$$C_N = \int \frac{\sigma_M}{\sigma_e} d\varepsilon \quad (2)$$

where  $\sigma_M$  is the maximum principal stress,  $\sigma_e$  is the effective stress,  $\varepsilon$  is the equivalent strain, and  $C_N$  is a critical value for fracture, above which the loss of metal cohesion occurs. By introducing the critical  $C_N$  value and element separation condition, the loss of material cohesion and billet cracking can be identified. In this case, the fracture steps and the maximum number of elements that can be deleted in each fracture step were defined. It must be noted that deleting failed elements will decrease the overall volume of the billet, so element deletion rules must be defined carefully.

## 4 Results and discussion

### 4.1 Relation between composition, hardness, and billet cracking

The billets of Alloys A to D failed during the equal channel angular pressing at room temperature. As shearing occurs when the billet passes through the theoretical shear plane, the billets cracked on this plane. The cracked billets of Alloys C and D are shown in Fig. 1. The simulation of billet cracking is shown in Fig. 1(c) that is in good coincidence with the observed cracks in these billets. Although lead content in Alloys A to C improves metal flow, it promotes cracking in the

severely deformed areas. The maximum solubility of lead in  $\beta$ -brass (lead-copper-zinc alloys) at forging temperatures is around 2%, but lead is insoluble in  $\beta$ -brass at all temperatures. Since lead has a lower melting point than other constituents of brass, it tends to migrate towards the grain boundaries. Consequently, the lead content will contribute to catastrophic cracking during severe plastic deformation [11].

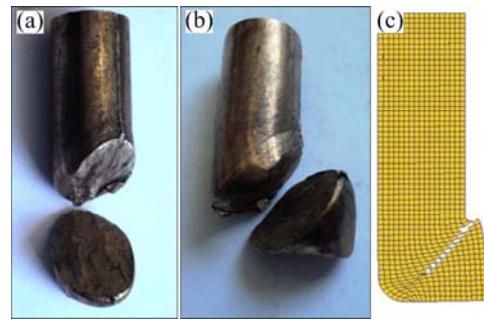


**Fig. 1** Cracked billets of Alloy C (a) and Alloy D (b) after processing by ECAP at room temperature, and simulation (c) of billet cracking by element separation method

In phosphor bronze (Alloy D), tin remains in the alpha copper solid solution and phosphorus forms copper phosphide phase. This alloy is more commonly constituted of a matrix of copper with tin in solid solution (soft alpha phase), a tin rich delta constituent, which is hard and interspersed throughout the matrix, and a hard phase of copper phosphide associated with the delta constituent, which is comparatively hard and brittle [12]. Therefore, the presence of tin-rich delta constituent, and hard phase of copper phosphide are the main reasons for limited formability of this alloy.

As Alloys A–D cracked at room temperature, they were processed by increasing the temperature up to 350 °C. Although increasing the temperature during ECAP is one of the useful methods to overcome cracking and segmentation, it leads to recrystallization, grain growth, and larger grain sizes. Therefore, the efficiency of ECAP for decreasing the average grain size and strengthening the samples according to Eq. (1) will be reduced. It is shown that lower ECAP temperature is more effective in grain refinement of different alloys because dynamic grain growth or dynamic/static recrystallization can be suppressed at lower temperatures [13–15]. Generally, the grain growth depends upon the nature of the microstructure of the material. For instance, in pure metals and solid-solution alloys, grain growth occurs rapidly at elevated temperatures in the absence of precipitates within the crystalline lattice, which restricts the movement of the grain boundaries. However, submicrometer grains are not affected by high temperatures in the materials containing

a distribution of fine precipitates in the matrix.

Figures 2(a) to (c) represent the billets of Alloys A to C processed by ECAP at 350 °C, for which cracking begins and develops on the top surface of the billet, because the maximum shear stress is applied on this surface. However, the cracks cannot propagate through

the total cross-section of the billet and they are actually stopped after propagating along half of the billet width. In addition, near the billet head, the sizes of cracks are larger than the rest of the billet, and by progressing the process, the cracks almost disappeared. This is mainly due to the back-pressure effect of the processed part of

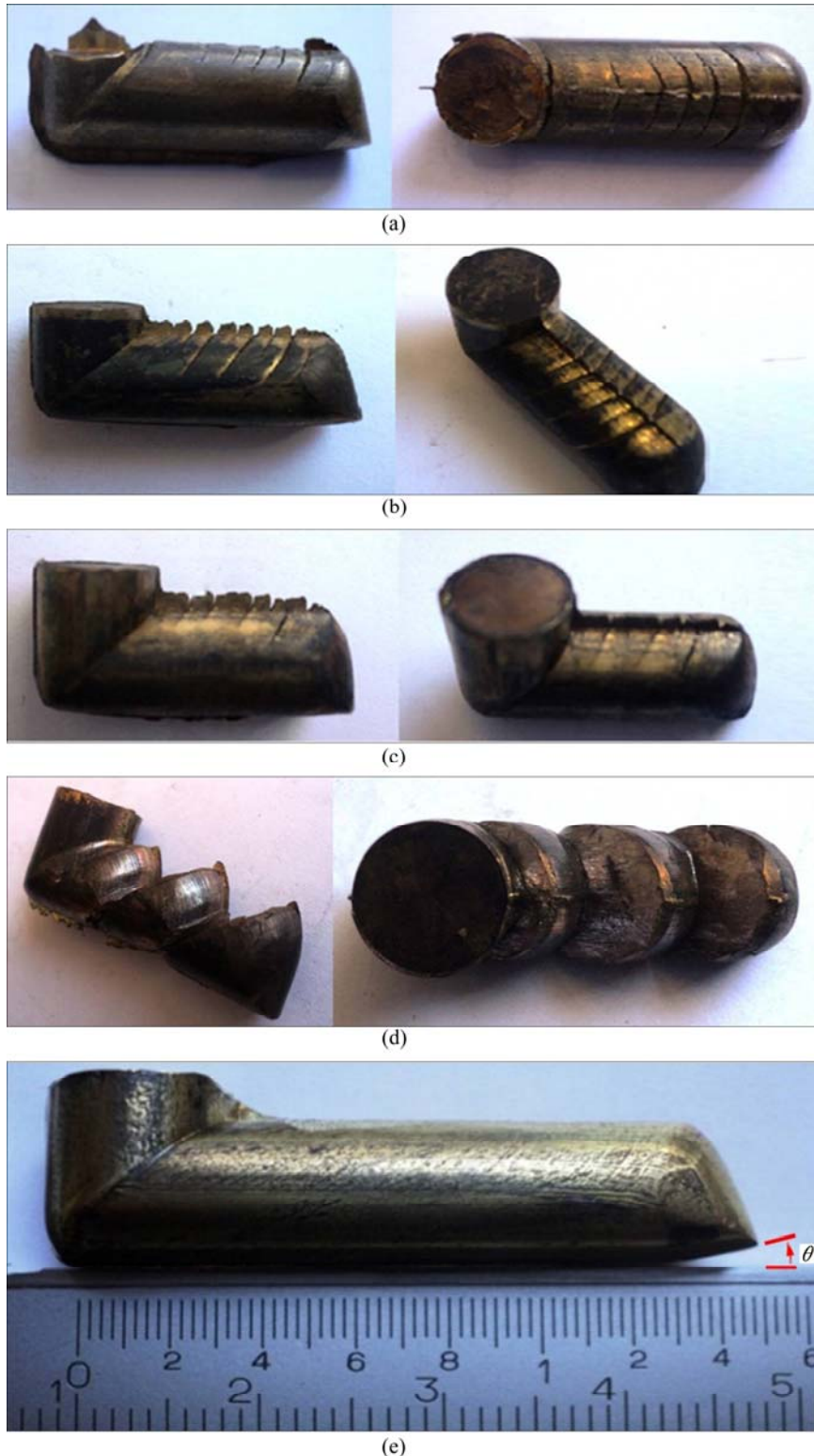


**Fig. 2** Appearance of samples after ECAP treatment: (a) Alloy A processed at 350 °C; (b) Alloy B processed at 350 °C; (c) Alloy C processed at 350 °C; (d) Alloy D processed at 350 °C; (e) Alloy E processed at room temperature

the billet. This observation shows excellent coincidence with the simulations by FIGUEIREDO et al [16] who showed that the accumulated damage is significantly reduced in the presence of back pressure, and only a small value of damage is observed along the top of the billet.

From Table 1, one can notice that Alloys A to C have Vickers microhardness of above HV 100. Therefore, billet cracking at room temperature and appearance of cracks on the top surface of the billet at 350 °C, seem to be directly proportional with the hardness of the alloy. Although Alloy D, which has a Vickers microhardness of HV 93 showed massive segmentation at 350 °C, the alloy retained its continuity. Figure 3 represents the billet of Alloy D processed by ECAP. It shows segmentation and continuous reduction and increase in the cross-sections of the billet after processing by ECAP, indicating the occurrence of flow softening. Similar phenomenon was reported by processing the extruded AZ31 magnesium alloy at 200 °C [5], annealed ZK60 magnesium alloy at 200–250 °C [5,7], commercially pure titanium at room temperature [17], and 4340 steel at 325 °C [17].

Neglecting the first crack on the billet head, the cracks on Alloys A and C (alpha/beta brasses) are smaller than that on the Alloy B, which contains lead and nickel. In this case, fine dispersion of the hard delta phase has a detrimental effect on achieving a perfect billet even at 350 °C.

Figure 2(e) illustrates the billet of Alloy E, which was successfully processed by ECAP at room temperature. Table 1 indicates that Alloy E has the minimum hardness (HV 86) among other samples. There are no signs of cracking and segmentation for the sample of the Alloy E and enhanced properties are expected, which will be discussed in further sections. Although many parameters are involved in cracking the billets, hardness seems to have a direct relation with segmentation during ECAP so that by decreasing the hardness, the possibility of segmentation is reduced.

The strain-rate sensitivity of the material also has a great influence on the flow localization. The increase in flow stress caused by the increase in strain rate may eliminate flow localization and formation of deformation bands in the processed billets. FIGUEIREDO et al [7] showed that increasing the strain-rate sensitivity of a material broadens the plastic deformation zone around the shear plane in ECAP. This may avoid the flow localization and formation of deformation bands in the processed billet. The unstable flow parameter in ECAP can be computed as follows [4]:

$$a = \frac{\gamma'}{m} \quad (3)$$

$$\gamma' = -\frac{\partial \ln \sigma}{\partial \ln \varepsilon} \quad (4)$$

where  $\gamma'$  is associated with the flow softening,  $m$  denotes the strain-rate sensitivity,  $\sigma$  represents the flow stress, and  $\varepsilon$  is the true strain. These equations imply that the increase in the strain-rate sensitivity may prevent the instability of plastic strain and localization during ECAP. It was also shown that the billet head shape during ECAP is directly dependent on the strain-rate sensitivity of the processed material, and the strain-rate sensitivity was altered by increasing the number of passes in ECAP [7]. However, in this work, different materials with different strain-rate sensitivities are assessed. Comparing the billet head rotation, Fig. 2(e) indicates that the strain-rate sensitivity of Alloy E is higher than that of the Alloys A to C. Furthermore, near-zero theta angle for Alloy D indicates the lowest strain-rate sensitivity for this alloy. These observations confirm that higher strain-rate sensitivity leads to improved formability of the alloy during ECAP and prevents the flow localization.

## 4.2 Simulation of billet cracking and segmentation

### 4.2.1 Influence of friction and processing speed

Figure 3 illustrates the sample of Alloy D, simulated in the processing condition similar to the experiments. The stress–strain diagram of copper alloy C51000 was entered to the FEM software, friction factor was chosen as 0.19 [18], processing speed was 10 mm/s, and normalized Cockcroft&Latham criterion was used to predict the damage. The final shape of the billet is very similar to the experiments, as shown in Fig. 3. This shows the capability of FEM to predict the shape of the billet and damage during ECAP. Therefore, it can be

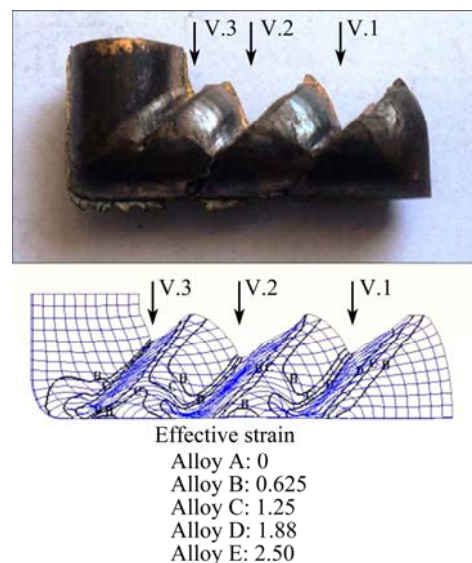


**Fig. 3** Simulation of massive segmentation of Alloy D subjected to ECAP (Blue lines show the material flow during deformation)

reliably used to predict the influence of different parameters on the damage evolution. However, proper considerations should be taken into account in FEM simulations. Similar to Alloys A to C, near the billet head, the sizes of segments are larger than those of the rest billets. In addition, the segments become smaller when the process is progressed. As anticipated, the back-pressure effect of the processed part of the billet reduces the depth of the formed V-shaped notches in the billet. As illustrated, the first and second notches (V.1 and V.2) have an equal depth approximately in both experiments and simulations. Nevertheless, the distance between two adjacent V-shaped notches and the depth of the third notch (V.3) decreased as the billets move through the channel. In experiments, the distance between V.2 and V.3 decreased by  $\sim 37.5\%$  compared with the distance between V.1 and V.2. In addition, the depth of V.3 is reduced by  $\sim 60.6\%$  compared with that of V.2. Similarly, in simulations, the distance between V.2 and V.3 is decreased by  $\sim 23.8\%$  compared with that between V.1 and V.2. Moreover, the depth of V.3 is reduced by  $\sim 43.2\%$  compared with that of V.2. Therefore, the numerical results show good coincidence with the experimental results.

In order to investigate the influence of friction and punch velocity, three friction factors of  $m=0$ ,  $m=0.19$ , and  $m=0.3$  were used [18]. In addition, the velocity ( $v$ ) was decreased from 10 to 0.5 mm/s. As can be seen in Figs. 4(a) to (c), the segments are stretched as the friction factor is increased. Furthermore, the shape of the billet is insensitive to the ram speed. This case was experimentally reported for pure titanium processed at room temperature for which all processing speeds of 0.5, 2.5, and 25 mm/s led to segmented flow of the material [17].

Changing the friction factors from 0 to 0.19 and 0.19 to 0.3 increases the distance between V.1 and V.2 by about 15.5% and 29.9%, respectively. In the meanwhile, the depth of V.1 increased by around 15.1% and 4.9% by changing the friction factors from 0 to 0.19, and 0.19 to 0.3, respectively. The influence of friction is more pronounced than the effect of punch velocity. Since, keeping the friction constant and decreasing the velocity from 10 to 0.5 mm/s increases the distance between V.1 and V.2, and depth of V.1 by only about 7.8% and 4.9%, respectively.

#### 4.2.2 Influence of back pressure

The influence of employing back pressure is shown in Fig. 5. Back pressure was increased in each step, up to achieving a uniform flow. It is demonstrated that the role of back pressure to obviate the formation of segments is much more pronounced than the effect of friction and punch velocity. In this case, employing a back pressure of around 600 MPa helps to obtain a billet without

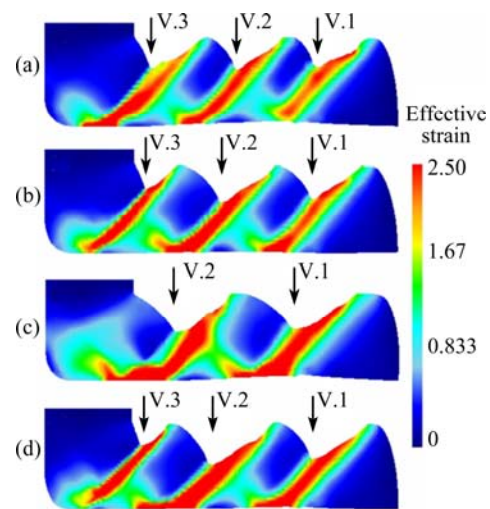


**Fig. 4** Massive segmentation of copper alloy under different processing conditions: (a)  $m=0$ ,  $v=10$  mm/s; (b)  $m=0.19$ ,  $v=10$  mm/s; (c)  $m=0.3$ ,  $v=10$  mm/s; (d)  $m=0.19$ ,  $v=0.5$  mm/s

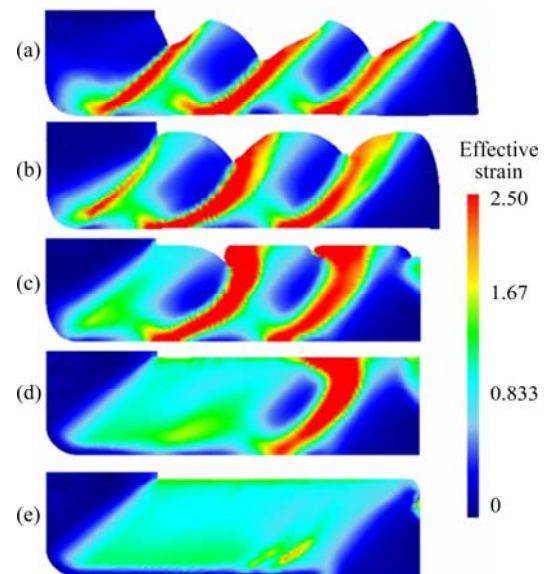


**Fig. 5** Obviation of segmentation in copper alloy at different back pressures: (a) 0 MPa; (b) 100 MPa; (c) 200 MPa; (d) 400 MPa; (e) 600 MPa

observable crack or segment. In this case, the induced strain profile is very similar to that of easy-to-work materials subjected to ECAP. It is well established that after processing the easy-to-work alloys by ECAP, a narrow region adjacent to the bottom surface experiences low strains [19,20]. However, the narrow region adjacent to the bottom surface of the billets, shown in Figs. 5(a) to (d), undergoes severe deformation in some areas, due to the strain localization and instabilities in material flow.

Figure 6 shows the force–time curves of Alloy D processed by ECAP, the occurrence of shear localization is associated with the flow softening and the load is decreased suddenly in the case of flow softening.

However, by increasing back pressure, the segments are diminished and a uniform force–time curve is achieved.

In the absence of back pressure, the punch load reaches a saturated level. Then, the billet segmentation causes a sudden drop in the required load for moving the billet through the exit channel. As the first V-shaped notch is formed (Fig. 5), the load is augmented gradually to another peak load, which is higher than the first peak. The load is then dropped after formation of the second notch, and this trend is continued. By increasing back pressure, as the segments are shrunk, the number of notches appeared in force–time curves decreased. Finally, a uniform force–time curve without localized flow is obtained.

Figure 7 represents the histograms of the effective

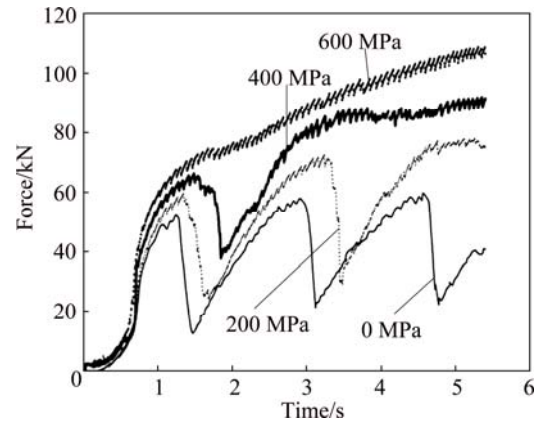


Fig. 6 Required force for processing Alloy D under different back pressures

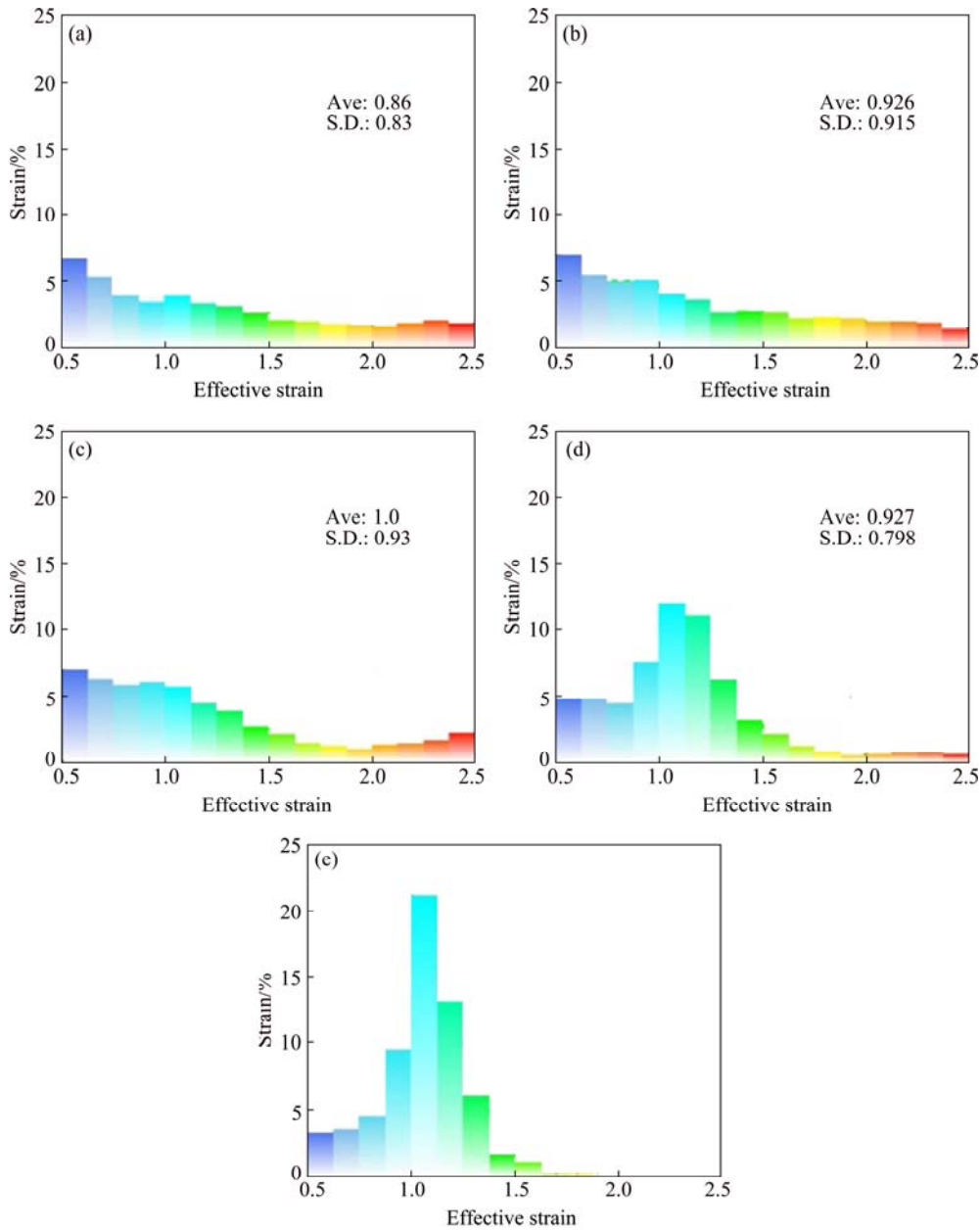


Fig. 7 Effective induced strain to billet of Alloy D under different back pressures: (a) 0 MPa; (b) 100 MPa; (c) 200 MPa; (d) 400 MPa; (e) 600 MPa

induced strain to the billets processed by different back pressures. As it was shown in the force–time curves, it is expected that diminishing the flow localization leads to a uniform strain distribution in the sample. This figure shows that, as back pressure increased, most regions of the billet experience a strain level of around 1. Although this figure shows the increase in the level of the homogeneity of the billet graphically, in order to evaluate the inhomogeneity index of the effective strain precisely, Eq. (5) was used to obtain the coefficient of variance of the equivalent plastic strain,  $\varepsilon^p$ .

$$\varepsilon^p = \frac{(\varepsilon_{S.D.}^p)}{\varepsilon_{ave}^p} \quad (5)$$

where  $\varepsilon_{ave}^p$  denotes the average of the equivalent plastic strain, and  $\varepsilon_{S.D.}^p$  stands for standard deviation of the equivalent plastic strain. The results are presented in Table 2. The inhomogeneity index fluctuates when the back pressure is less than 200 MPa. However, increasing back pressure from 0 to 400 MPa, and 600 MPa increases the billet homogeneity up to 7.5%, and 36.1%, respectively.

**Table 2** Calculation of inhomogeneity of induced strain

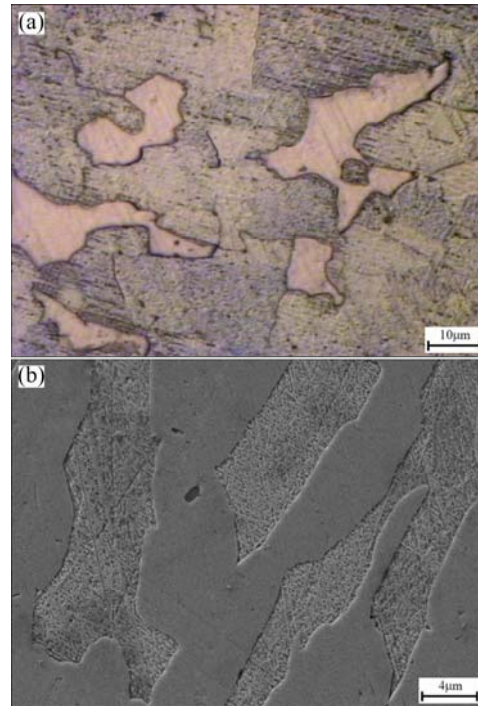
Back pressure/MPa	Average strain	Standard deviation	Inhomogeneity index
0	0.860	0.830	0.97
100	0.926	0.915	0.99
200	1.000	0.930	0.93
400	0.927	0.798	0.86
600	0.740	0.460	0.62

### 4.3 Properties of Alloy E after ECAP

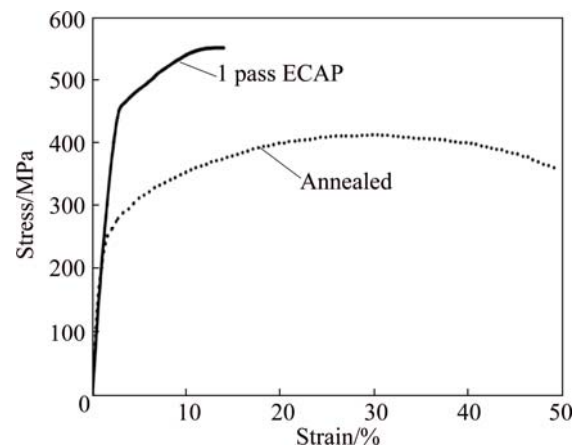
The main purpose of using ECAP is obtaining a work-piece without visible sign of crack or segment. In this case, achieving a refined microstructure strengthens the work-piece or provides better superplastic forming characteristic. Figure 8 shows the typical microstructure of Alloy E before and after ECAP treatment observed by optical microscopy (OM) and scanning electron microscopy (SEM), respectively. It can be seen that the average grain size reduces after only one ECAP pass. As more than 99% of grain refinement [21], and more than 95% of strengthening of the work-piece occurs only after one pass of SPD process [22], attaining a perfect billet after the first pass is of great interest. In addition, cracked billets cannot be used in further processing steps.

Figure 9 illustrates the engineering stress–strain curves for the sample of Alloy E before and after ECAP. As shown in this figure, the yield and the ultimate strengths show drastic increase after only one pass of ECAP. However, the elongation to failure is reduced simultaneously. Around 68.4% increase in the yield

stress accompanied by about 71.8% decrease in the ductility was observed after only one ECAP pass. The dislocation accumulation is more difficult in ultra-fine grained and nanostructured materials because the small grain size restricts the dislocation glide when a dislocation emanates from a grain boundary. Since the grain size is very small, dislocation may be deposited at another grain boundary without intersecting other dislocations. In this way, different mechanical properties are altered [23].



**Fig. 8** OM image of Alloy E before ECAP (a) and SEM image of Alloy E after one ECAP pass (b)



**Fig. 9** Engineering stress–strain curves before and after ECAP

## 5 Conclusions

1) ECAP process was conducted on five commercial Cu-based alloys. Billet cracking at room

temperature and appearance of cracks on the top surface of the billets at 350 °C, were directly proportional with the hardness of the alloys and their constitutive phases. In addition, it was not possible to perform ECAP on alpha/beta brasses even at a temperature of 350 °C.

2) Numerical simulation of segmentation of Alloy D showed a good coincidence with the experimental results. Then, it was used to predict the effect of different parameters on shear localization. The segments were stretched as friction factor was increased. In addition, the shape of the billet was insensitive to ram speed. Furthermore, the role of back pressure in obviating the formation of segments was much more pronounced than the effect of friction and punch velocity. In this case, employing a back pressure of around 600 MPa led to obtaining a billet without observable crack or segment.

3) Diminishing the flow localization using back pressure, led to a uniform strain distribution in the billet. The billet homogeneity was increased up to 7.5%, and 36.1%, when back pressure was increased from 0 to 400 and 600 MPa, respectively.

4) Successful processing of Alloy E by ECAP treatment led to significant grain refinement after only one pass. Consequently, around 68.4% increase in the yield stress accompanied by about 71.8% decrease in the ductility was observed.

## Acknowledgments

The authors would like to thank Young Researchers and Elite Club, Birjand Branch, Birjand, Iran, and K. N. Toosi University of Technology, Tehran, Iran, for financial support and providing research facilities used in this work.

## References

- [1] LANGDON T. The mechanical properties of superplastic materials [J]. *Metallurgical Transactions A*, 1982, 13(5): 689–701.
- [2] JIANG J H, MA A B, SAITO N, WATAZU A, LIN P H, NISHIDA Y. Effect of microstructures on superplasticity of Al–11%Si alloy [J]. *Transactions of Nonferrous Metals Society of China*, 2007, 17(3): 509–513.
- [3] VALIEV R Z, LANGDON T G. Principles of equal-channel angular pressing as a processing tool for grain refinement [J]. *Progress in Materials Science*, 2006, 51(7): 881–981.
- [4] SEMIATIN S L, DELO D P, SEGAL V M, GOFORTH R E, FREY N D. Workability of commercial-purity titanium and 4340 steel during equal channel angular extrusion at cold-working temperatures [J]. *Metallurgical and Materials Transactions A*, 1999, 30(5): 1425–1435.
- [5] CETLIN P, AGUILAR M, FIGUEIREDO R, LANGDON T. Avoiding cracks and inhomogeneities in billets processed by ECAP [J]. *Journal of Materials Science*, 2010, 45(17): 4561–4570.
- [6] FIGUEIREDO R B, CETLIN P R, LANGDON T G. The evolution of damage in perfect-plastic and strain hardening materials processed by equal-channel angular pressing [J]. *Materials Science and Engineering A*, 2009, 518(1–2): 124–131.
- [7] FIGUEIREDO R B, CETLIN P R, LANGDON T G. The processing of difficult-to-work alloys by ECAP with an emphasis on magnesium alloys [J]. *Acta Materialia*, 2007, 55(14): 4769–4779.
- [8] SEMIATIN S L, DELO D P, SHELL E B. The effect of material properties and tooling design on deformation and fracture during equal channel angular extrusion [J]. *Acta Materialia*, 2000, 48(8): 1841–1851.
- [9] DENG W J, XIA W, TANG Y. Finite element simulation for burr formation near the exit of orthogonal cutting [J]. *The International Journal of Advanced Manufacturing Technology*, 2009, 43(9–10): 1035–1045.
- [10] OH S I, CHEN C C, KOBAYASHI S. Ductile fracture in axisymmetric extrusion and drawing. Part 2: Workability in extrusion and drawing [J]. *Journal of Engineering for Industry*, 1979, 101(1): 36–44.
- [11] COMMITTEE A H. *Metals handbook: Forming and forging* [M]. Metals Park, Ohio: American Society for Metals, 1978.
- [12] HABASHI F. *Alloys: Preparation, properties, applications* [M]. USA: Wiley, 2008.
- [13] KIM W J, JEONG H T. Grain-size strengthening in equal-channel-angular-pressing processed AZ31 Mg alloys with a constant texture [J]. *Materials Transactions*, 2005, 46(2): 251–258.
- [14] HUANG C X, YANG G, GAO Y L, WU S D, ZHANG Z F. Influence of processing temperature on the microstructures and tensile properties of 304L stainless steel by ECAP [J]. *Materials Science and Engineering A*, 2008, 485(1–2): 643–650.
- [15] STOLYAROV V V, ZHU Y T, LOWE T C, VALIEV R Z. Microstructures and properties of ultrafine-grained pure titanium processed by equal-channel angular pressing and cold deformation. [J]. *Journal of Nanoscience and Nanotechnology*, 2001, 1(2): 237–242.
- [16] FIGUEIREDO R, CETLIN P, LANGDON T. Stable and unstable flow in materials processed by equal-channel angular pressing with an emphasis on magnesium alloys [J]. *Metallurgical and Materials Transactions A*, 2010, 41(4): 778–786.
- [17] SEMIATIN S L, DELO D P. Equal channel angular extrusion of difficult-to-work alloys [J]. *Materials & Design*, 2000, 21(4): 311–322.
- [18] SHOKUHFAAR A, NEJADSEYFI O. The influence of friction on the processing of ultrafine-grained/nanostructured materials by equal-channel angular pressing [J]. *Journal of Materials Engineering and Performance*, 2014, 23(3): 1038–1048.
- [19] PRELL M, XU C, LANGDON T G. The evolution of homogeneity on longitudinal sections during processing by ECAP [J]. *Materials Science and Engineering A*, 2008, 480(1–2): 449–455.
- [20] HU H J, ZHANG D F, PAN F S. Die structure optimization of equal channel angular extrusion for AZ31 magnesium alloy based on finite element method [J]. *Transactions of Nonferrous Metals Society of China*, 2010, 20(2): 259–266.
- [21] GENDELMAN O V, SHAPIRO M, ESTRIN Y, HELLMIG R J, LEKHTMAKHER S. Grain size distribution and heat conductivity of copper processed by equal channel angular pressing [J]. *Materials Science and Engineering A*, 2006, 434(1–2): 88–94.
- [22] ALHAJERI S N, GAO N, LANGDON T G. Hardness homogeneity on longitudinal and transverse sections of an aluminum alloy processed by ECAP [J]. *Materials Science and Engineering A*, 2011, 528(10–11): 3833–3840.
- [23] SUN P L, CERRETA E K, BINGERT J F, GRAY III G T, HUNDLEY M F. Enhanced tensile ductility through boundary structure engineering in ultrafine-grained aluminum [J]. *Materials Science and Engineering A*, 2007, 464(1–2): 343–350.

## 等径角挤压铜合金的分节断裂

Omid NEJADSEYFI<sup>1</sup>, Ali SHOKUH FAR<sup>1</sup>, Vahid MOODI<sup>2</sup>

1. Advanced Materials and Nanotechnology Research Lab, Faculty of Mechanical Engineering, K. N. Toosi University of Technology, Tehran, Iran;
2. Young Researchers and Elites Club, Birjand Branch, Islamic Azad University, Birjand, Iran

**摘 要:** 本研究提供了等径角挤压不同铜合金的局部剪切、坯锭开裂和分节断裂的实验依据。结果表明, 尽管很多参数影响局部剪切, 但是合金的硬度和分节断裂与其有着直接的关系, 而硬度与合金的成分和相组成有关。在室温下,  $\alpha$ -黄铜可以成功进行等径角挤压, 而  $\alpha/\beta$  黄铜甚至在 350 °C 下都不能成功进行等径角挤压。利用 DEFORM<sup>TM</sup> 软件模拟了开裂和分节断裂, 研究不同参数对分节断裂的影响。结果表明, 摩擦力和加工速率对获得完美坯锭影响很小, 而利用背压可以很好地减小局部剪切、坯锭裂纹、分节断裂和破坏。利用背压能减小流动局部化, 当背压由 0 提高到 600 MPa 时, 可以提高材料流动均匀性并且使坯锭的均匀性提高 36.1%。

**关键词:** 背压; 黄铜; 青铜; 破坏; 流动局部化; 应力-应变行为; 拉伸强度; 延展性

(Edited by Xiang-qun LI)